Interplanetary magnetic field control of afternoon-sector detached proton auroral arcs

J. L. Burch,[1] W. S. Lewis,[1] T. J. Immel,[2] P. C. Anderson,[3] H. U. Frey,[2] S. A. Fuselier,[4] J.-C. Gérard,[5] S. B. Mende,[2] D. G. Mitchell,[6] and M. F. Thomsen[7]

Received 18 September 2001; revised 21 December 2001; accepted 21 December 2001; published 25 September 2002.

[1] Data from the Far Ultraviolet Imager (FUV) on the Imager for Magnetopause-to-Aurora Global Exploration (IMAGE) satellite show that subauroral proton arcs appear in the afternoon sector during geomagnetically disturbed periods when the interplanetary magnetic field rotates either from south to north or from west to east and when the magnetosphere is moderately compressed. Time series of proton aurora images show that the proton emissions are generally aligned along the equatorward part of the auroral oval. However, when interplanetary magnetic field (IMF) B_z changes from negative to positive the auroral oval contracts toward higher latitudes while the ring current proton precipitation remains stationary, resulting in a separation of several degrees between the latitude of the new oval position and a subauroral proton arc in the afternoon sector. A similar effect occurs when IMF B_y rotates from negative to positive, in which case the oval in the afternoon sector retreats toward higher latitudes, again leaving a separation between the oval and the subauroral proton arc of several degrees. Comparisons with low-altitude and geosynchronous satellite data show that the subauroral proton arc is caused by the precipitation of protons with energies from several keV to 30 keV and is likely associated with the existence of a plasmaspheric ''drainage plume.'' In contrast, the proton emissions along the main oval are caused by protons with energies generally less than 10 keV. *INDEX TERMS:* 2704 Magnetospheric Physics: Auroral phenomena (2407); 2736 Magnetospheric Physics: Magnetosphere/ionosphere interactions; 2716 Magnetospheric Physics: Energetic particles, precipitating; *KEYWORDS:* auroral phenomena, magnetosphere/ionosphere interactions, auroral ionosphere, particle precipitation

Citation: Burch, J. L., W. S. Lewis, T. J. Immel, P. C. Anderson, H. U. Frey, S. A. Fuselier, J.-C. Gérard, S. B. Mende, D. G. Mitchell, and M. F. Thomsen, Interplanetary magnetic field control of afternoon-sector detached proton auroral arcs, *J. Geophys. Res.*, *107*(A9), 1251, doi:10.1029/2001JA007554, 2002.

1. Introduction

[2] The proton component of the aurora was identified a little over a half century ago on the basis of hydrogen Balmer emissions detected from the ground. Attributed by their discoverer to ''occasional showers of hydrogen or a kind of 'hydrogen radiation' occasionally coming from the sun'' [*Vegard*, 1939], the observed Hα and Hβ lines were later determined to be Doppler-shifted emissions from excited neutral hydrogen atoms produced by charge exchange between precipitating protons and the neutral constituents of the upper atmosphere [*Vegard*, 1948; *Meinel*, 1951]. (The early work on the proton aurora, from its discovery through the late 1960s, is reviewed by *Eather* [1967].) Subsequent studies of the proton aurora have been based on ground-based optical observations of auroral Hα and Hβ emissions as well as of emissions at other wavelengths [e.g., *Ono et al.*, 1987; *Lorentzen and Moen*, 2000; *Takahashi and Fukunishi*, 2001] and on in situ measurements of auroral protons with rocket- and satellite-borne particle detectors [e.g., *Miller and Whalen*, 1976; *Hardy et al.*, 1989]. In addition, limb-imaging data on proton/hydrogen emissions from spectrographic imagers on the Midcourse Space Experiment (MSX) satellite have recently been reported [*Strickland et al.*, 2001].

[3] Ground-based optical data and space-based particle measurements are necessarily restricted in their spatial and/or temporal coverage. However, global proton precipitation patterns (and hence the global morphology of the proton aurora) have been derived statistically for different levels of geomagnetic activity from the extensive database of ion measurements made by Defense Meteorological Satellite Program (DMSP) satellites [*Hardy et al.*, 1989]. These data reveal a C-shaped region of maximum energy flux on the night side, a maximum in average particle energy in the

[1]Southwest Research Institute, San Antonio, Texas, USA.
[2]University of California, Berkeley, California, USA.
[3]Aerospace Corporation, El Segundo, California, USA.
[4]Lockheed Martin Advanced Technology Center, Palo Alto, California, USA.
[5]University of Liège, Liège, Belgium.
[6]Applied Physics Laboratory, Johns Hopkins University, Laurel, Maryland, USA.
[7]Los Alamos National Laboratory, Los Alamos, New Mexico, USA.

0148-0227/02/2001JA007554$09.00

evening sector, and a maximum in integrated number flux in the cusp region. Comparison of the proton precipitation patterns with those derived from DMSP particle data for auroral electron precipitation [*Gussenhoven et al.*, 1983] shows that the proton oval is shifted equatorward of the electron oval in the evening sector and slightly poleward of it in the morning sector.

[4] The study by Hardy et al. has contributed greatly to our knowledge of the global pattern of proton precipitation; however, statistical models cannot adequately capture the rapid spatial and temporal variations in auroral emission intensity and morphology that occur during magnetospheric disturbances. For this, as was demonstrated by the significant advances in our understanding of the electron aurora achieved with the auroral images obtained with the Dynamics Explorer 1 imaging photometers [*Frank and Craven*, 1988], global imaging of the auroral oval with adequate time resolution is required.

[5] Global imaging of the proton aurora is now routinely provided by the Far-Ultraviolet (FUV) Spectrographic Imager (SI) on the Imager for Magnetopause-to-Aurora Global Exploration (IMAGE) spacecraft, which was launched on 25 March 2000 into an orbit with 90° inclination, geocentric apogee of 8.2 R_E, and initial perigee altitude of 1000 km [*Burch*, 2000]. The FUV-SI [*Mende et al.*, 2000] is a grating-based spectrometer with two channels. The SI12 channel produces global images of Earth's proton aurora by detecting Doppler-shifted Lyman α emissions (121.8 nm) from energetic neutral hydrogen atoms created through charge exchange between energetic (several keV) precipitating protons and thermospheric neutral atoms. The signal in the second channel, SI13, is mostly ($\sim$60%) from 135.6 nm emissions from atomic oxygen. By observing at the red-shifted Lyman α wavelength of 121.8 ± .1 nm, the SI eliminates most of the background of unshifted solar Lyman α (121.6 nm) emitted by exospheric hydrogen, making it possible to image dayside as well as nightside proton emissions. With an exposure time of 5 s and an imaging cadence of two minutes, as determined by the spacecraft spin period, the SI is well able to track, with good temporal resolution, the dynamical evolution of the proton aurora over a period of several hours before and after apogee.

[6] The study of the global morphology and dynamics of the proton aurora revealed in the SI12 images, and of their relation to the morphology and dynamics of the electron aurora as well as to magnetospheric and interplanetary conditions, is only now beginning [*Burch et al.*, 2001; *Frey et al.*, 2001; *Mende et al.*, 2001; *Immel et al.*, 2002; *Gérard et al.*, 2001]. Here we describe the development of detached subauroral proton arcs in the afternoon and dusk sectors of the northern hemisphere under changing IMF conditions. Regions of detached proton precipitation equatorward of the main proton oval observed in particle data have been reported by *Sanchez et al.* [1993] and *Gvozdevsky et al.* [1997]. Further, features similar to those reported here, subauroral detached arcs and patches in the dusk/evening sector equatorward of the diffuse oval, were observed at 557.7 and 391.4 nm with the Auroral Scanning Photometer (ASP) on board ISIS 2 [*Anger et al.*, 1978; *Moshupi et al.*, 1979]. ISIS particle data, however, indicated that these structures were excited by electron rather than ion precipitation [*Wallis et al.*, 1979].

[7] In this paper we describe two events during which detached subauroral proton arcs were observed in the afternoon sector. Both events occurred during periods of moderate to intense substorm activity (*AE* values from a few hundred to over 1000 nT) and at times when the solar wind dynamic pressure was enhanced and the magnetosphere moderately compressed. In the first case, the subauroral arc appeared during a south-to-north IMF rotation, which caused the main proton oval to contract poleward, leaving the apparently preexisting proton arc in the equatorward part of the oval at its original latitude. The second event is similar, except that the subauroral arc appears during a rotation of the IMF from westward to eastward. In this case the afternoon-sector oval moves poleward, as predicted by *Burch et al.* [1985] (in terms of the merging line) and *Cowley et al.* [1991] (in terms of the open-closed field line boundary), again revealing a subauroral arc, which appears from the image sequences to have pre-existed in the equatorward part of the proton oval before the IMF B_y rotation. DMSP particle data show: (1) precipitating energetic ions ($\sim$3–30 keV) over the detached arc and (2) precipitation of lower-energy ions (<10 keV) over the contracting proton auroral oval. In addition, geosynchronous spacecraft data available for one of the events show the existence of a plasmaspheric drainage plume with cold plasma vortical oscillations with at periods of about 10 min at the same Λ-MLT location as the proton arc.

2. Observations

[8] Subauroral proton emissions have been observed with the SI12 instrument on a number of occasions [cf. *Immel et al.*, 2002]. In this section we present observations of two events in which the IMF influence on the development of the proton arc is readily apparent: one on 9–10 November 2000 and the other on 23–24 January 2001. The January event is discussed by *Immel et al.* [2002], who have established that the detached subauroral arcs were produced by protons with mean energies of 20–30 keV measured in the southern conjugate hemisphere in a region essentially devoid of electron precipitation.

2.1. The 9–10 November 2000 Event

[9] SI12 proton aurora images acquired between 2329:22 UT on 9 November and 0200:35 UT on 10 November recorded the development of a detached subauroral arc. Figure 1 shows a subset of the images obtained during this period (every other image from the selected time interval is shown). A clear poleward contraction of the proton auroral oval of several degrees of invariant latitude can be seen by comparing the images at 2339:35 UT (upper left image) and at 0057:16 (lower right image). The first hint of a detachment of what eventually becomes a subauroral arc can be seen in the sixth image (0000:02) where a "spur" has developed near 1930 MLT. As time goes on, the rest of the detaching arc becomes more localized in the mid-afternoon sector. But during this time the latitude of the detached arc stays nearly constant, with the primary motion being the poleward contraction of the main part of the auroral oval. During the poleward contraction of the proton oval the intensity of the

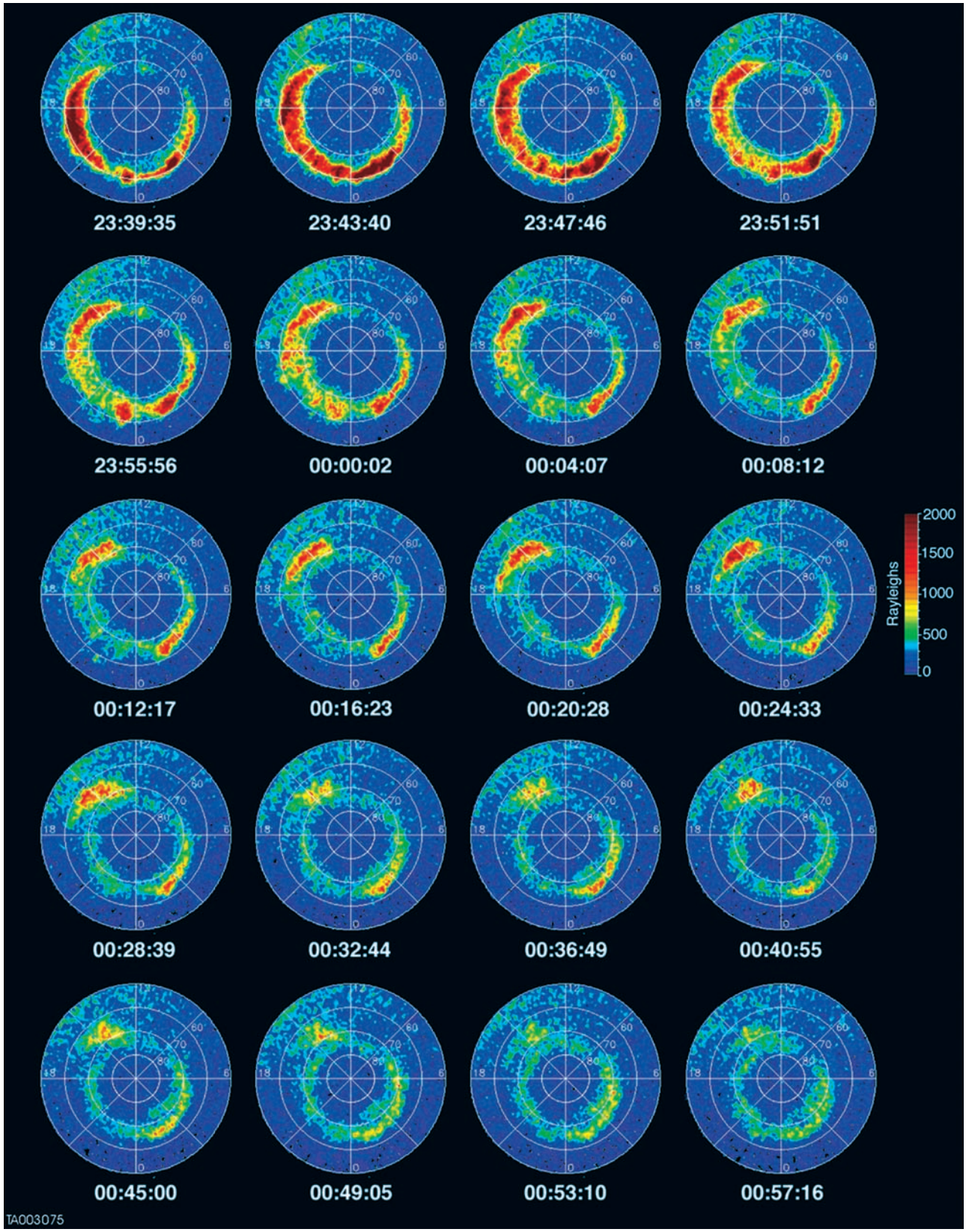

Figure 1. Proton aurora images on 9–10 November 2000. Times shown are in universal time. Pixels have been mapped into Λ-MLT coordinates. Noon is at the top. The false color indicates the emission intensity in Rayleighs.

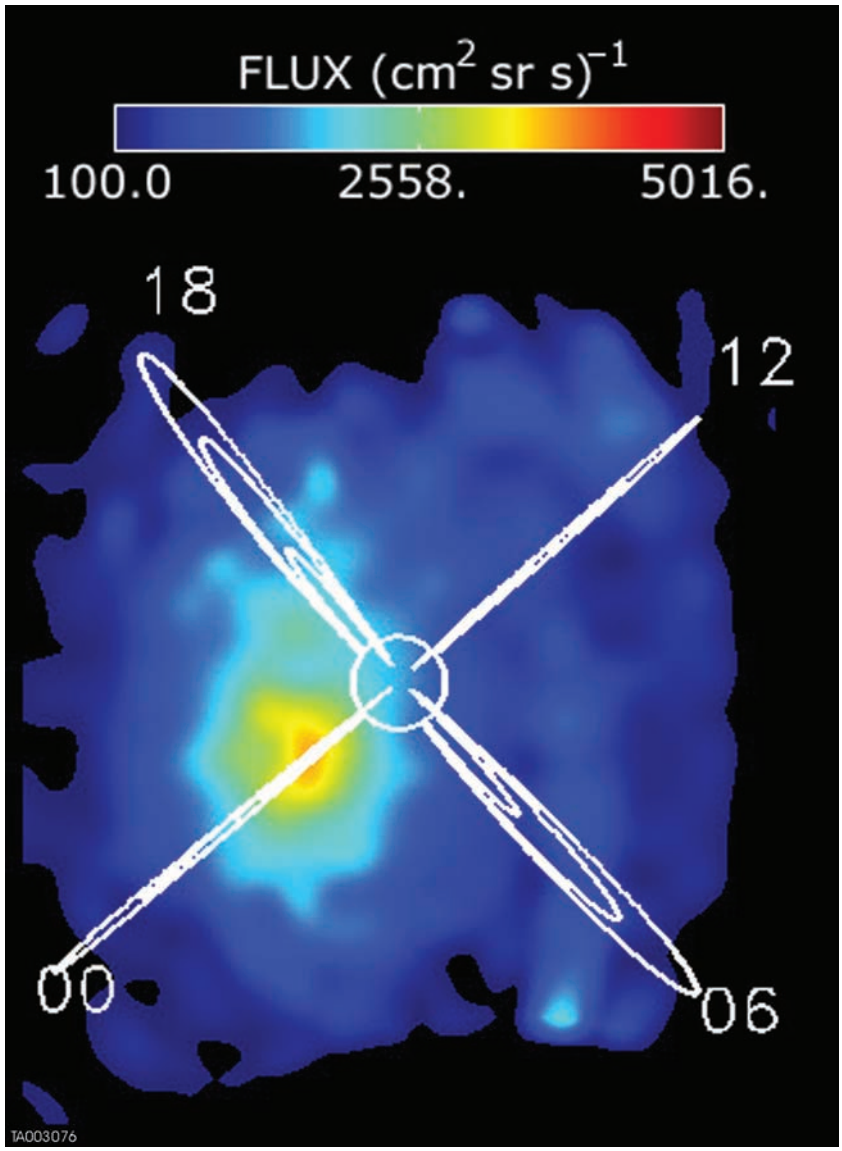

Figure 2. HENA image showing neutral atom fluxes in the 10–60 keV energy range. The data shown were acquired on 10 November 2000, between 0027:07 and 0029:07 UT (during one 2-min spacecraft spin period). The spacecraft was near apogee, at a geocentric distance of 7.8 R_E. The view is toward the north pole. The Earth is represented by the white circle. Representative fields lines extending to radial distances of 4, 8, and 12 R_E are shown at noon, dusk, midnight, and dawn. The image shows a typical substorm distribution of energetic particles during the time of the 9–10 November substorm event.

night-side emissions decreases markedly, indicating a diminished level of proton injections. The arc persists, increasingly attenuated, until ~0145 UT. Another prominent feature seen in the first image, and reappearing in most several of the other images is the cusp (small circle near 1100 MLT and poleward of the oval). *Fuselier et al.* [2002] have identified this type of feature as characteristic of cusp proton precipitation during periods of northward IMF.

[10] A severe magnetic storm, with a *Dst* minimum of −159 nT, had occurred 3 days earlier, triggered by a CME that passed the Advanced Composition Explorer (ACE) spacecraft at 0914 UT on 6 November. By 9 November, however, the ring current had recovered; and although geomagnetic conditions were active (Kp = 4) at the time of the subauroral arc event, they did not reach the level of a minor magnetic storm (Kp = 5), as defined by the NOAA Space Weather Scales. The *Dst* index at the time of the November event was negative but remained greater than −20 nT. There was significant substorm activity at the time of the event, with *AE* reaching values near 1000 nT. The detached arc appeared during the substorm recovery phase, as *AE* was decreasing from its maximum value. Images from the IMAGE High-Energy Neutral Atom (HENA) imager [*Mitchell et al.*, 2000] obtained during 9–10 November event (Figure 2) showed a typical substorm injection of protons (10–60 keV), with the strongest ENA emissions extending from ~1700 MLT through midnight to ~0200 MLT.

[11] IMF data were available from the ACE spacecraft for 9 and 10 November and are shown in Figure 3. ACE

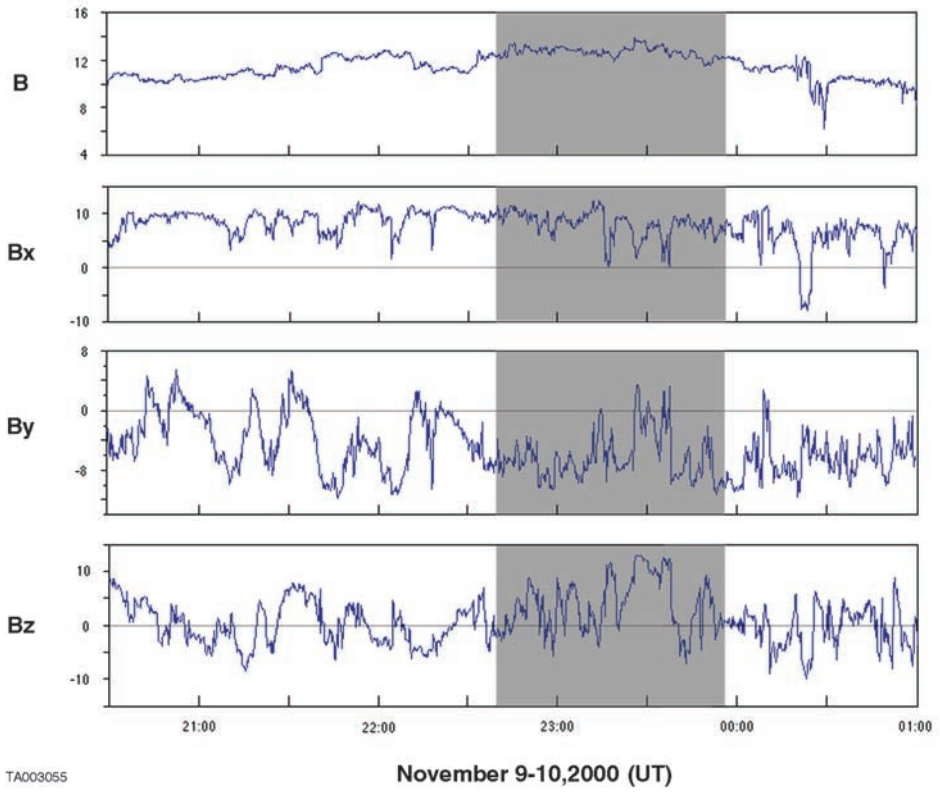

Figure 3. ACE IMF data in GSM coordinates for 9–10 November 2000. The shaded region shows the time period covered by the images in Figure 1 after applying a one-hour transit time correction from ACE.

velocity, temperature, and density readings were not available owing to sensor contamination associated with a solar proton event; however, data from the CELIAS proton monitor on the SOHO spacecraft indicate that the solar wind velocity and density were somewhat elevated (V_{sw} = 574 km s^{-1} and n_p = 9.3 cm^{-3}). Force balance calculations show that the magnetosphere was moderately compressed on the dayside, with the nose of the magnetopause predicted to be located at 7.3 R_E geocentric. The shaded region shows the time period covered by the images in Figure 1 after applying a one-hour transit time correction from ACE. We note that B_x was fluctuating but remained positive, B_y was fluctuating but

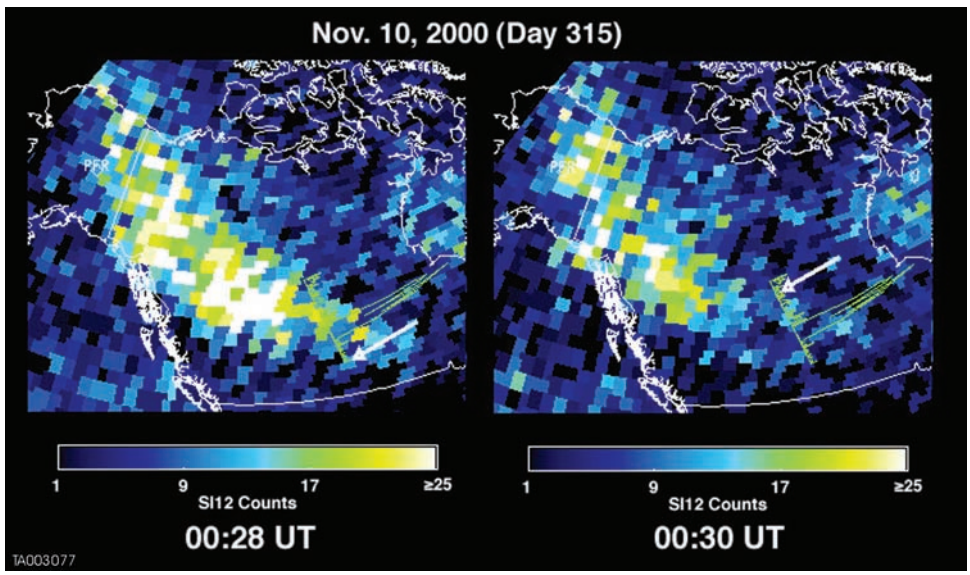

Figure 4. Plot showing the segment of the DMSP 13 orbit that passes through the end of the subauroral proton arc at 0028 UT. Two minutes later, at 0030 UT, the arc has moved and the spacecraft no longer sees a strong proton precipitation feature. The location of the spacecraft at each time is indicated by the arrow.

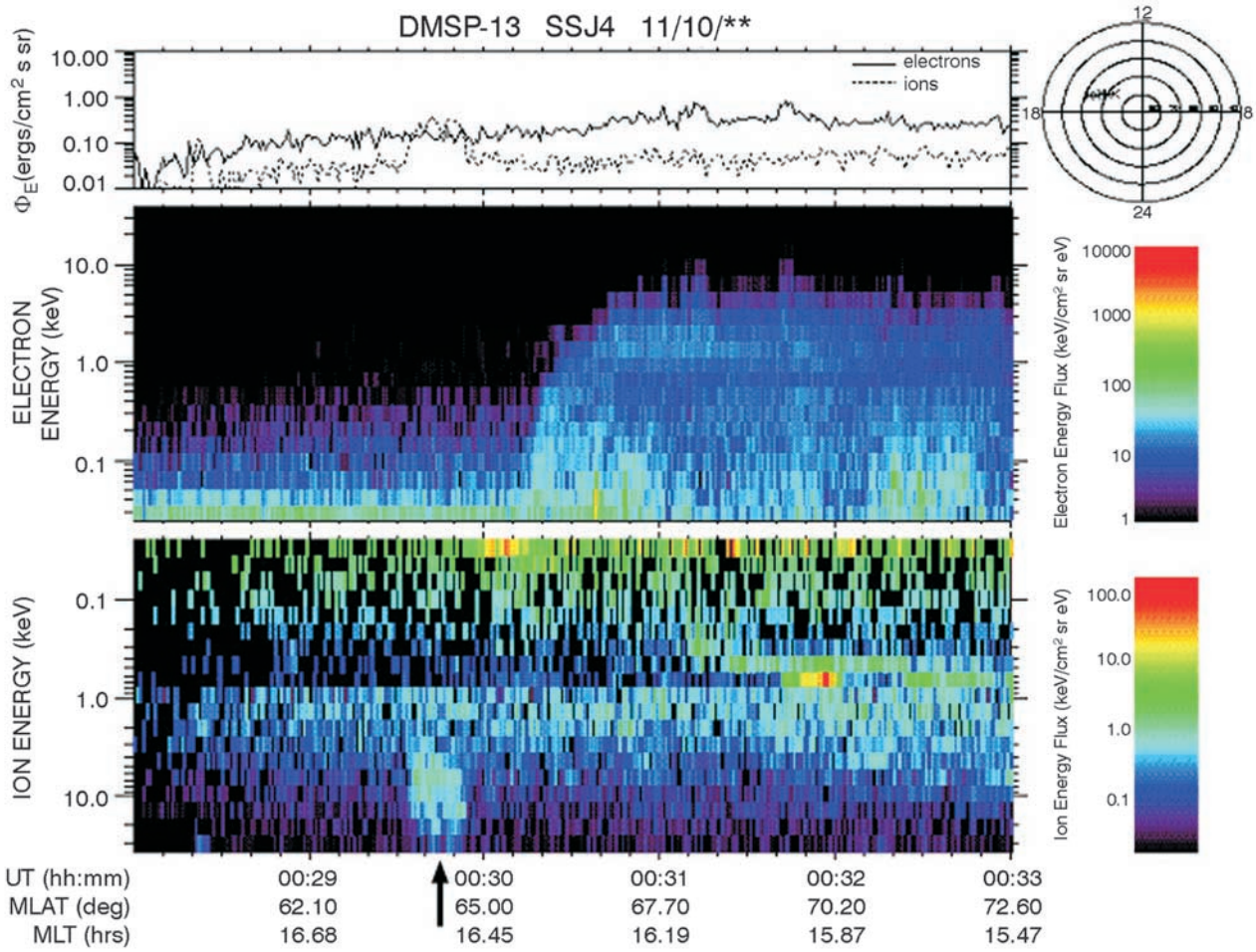

Figure 5. DMSP 13 particle data for 10 November 2000. The black arrow points to the precipitation feature in the ion panel that is associated with subauroral arc. No comparable feature is seen in the electron panel (top), indicating that ion (proton) precipitation rather than electron precipitation is responsible for the detached arc. The spacecraft track for the time period shown is indicated in the polar plot in the upper right-hand corner.

remained generally negative, while B_z attained high positive values (exceeding 10 nT) compared to values before and after the shaded interval, which were fluctuating over positive and negative values centered approximately at zero. The maximum values of B_z occurred around 2330 UT at ACE (~0030 UT on 10 November at the Earth), which is near the middle of the set of images in Figure 1 where the detached arc has become most prominent.

[12] The DMSP-13 spacecraft crossed over the detached arc at approximately 0029:35 to 0029:55 UT on 10 November (Figure 4). The DMSP electron and proton precipitation data are shown in Figure 5. During this time period a strong proton precipitation feature is seen in the DMSP spectrogram with the energy flux reaching ~0.12 ergs cm^{-2} s^{-1} sr^{-1} over an energy range between 3 and 30 keV. The proton fluxes were located equatorward of the diffuse electron fluxes and were accompanied only by photoelectrons with energies less than a few hundred eV. The DMSP proton fluxes were centered at $\Lambda \sim 64°$ and MLT ~ 16.5 hrs, which is consistent with the proton arc location in Figure 1 (0028:39 UT). As shown in Figure 5, the proton fluxes poleward of the detached arc remained low in energy and intensity until near the end of the period plotted, by which time energy fluxes approached ~0.06 cm^{-2} s^{-1} sr^{-1} and ion energies were in the few keV range where they are visible in the SI-12 channel. This location ($\Lambda \sim 72°$) corresponds to the location of the weak emissions along the main auroral oval shown in Figure 1.

2.2. The 23–24 January 2001 Event

[13] Data from another detached proton arc event observed between 2259:04 UT on 23 January and 0024:59 UT on 24 January are presented in Figure 6. Again, only a subset of the images acquired during this period is shown. Two images are shown for each time: (1) the image in geographical coordinates as seen from the IMAGE spacecraft, and (2) a Λ-MLT mapping of the same pixels. The ring current was generally quiet on this day, although minor storm levels had been approached briefly between 1800 and 2100 UT (Kp = 5–). Geomagnetic conditions were active (Kp = 4) at the time of the event, which occurred during the last of a continuous series of substorms on that day that had begun at about 1420 UT. As in the 9–10 November case, the arc appears during the

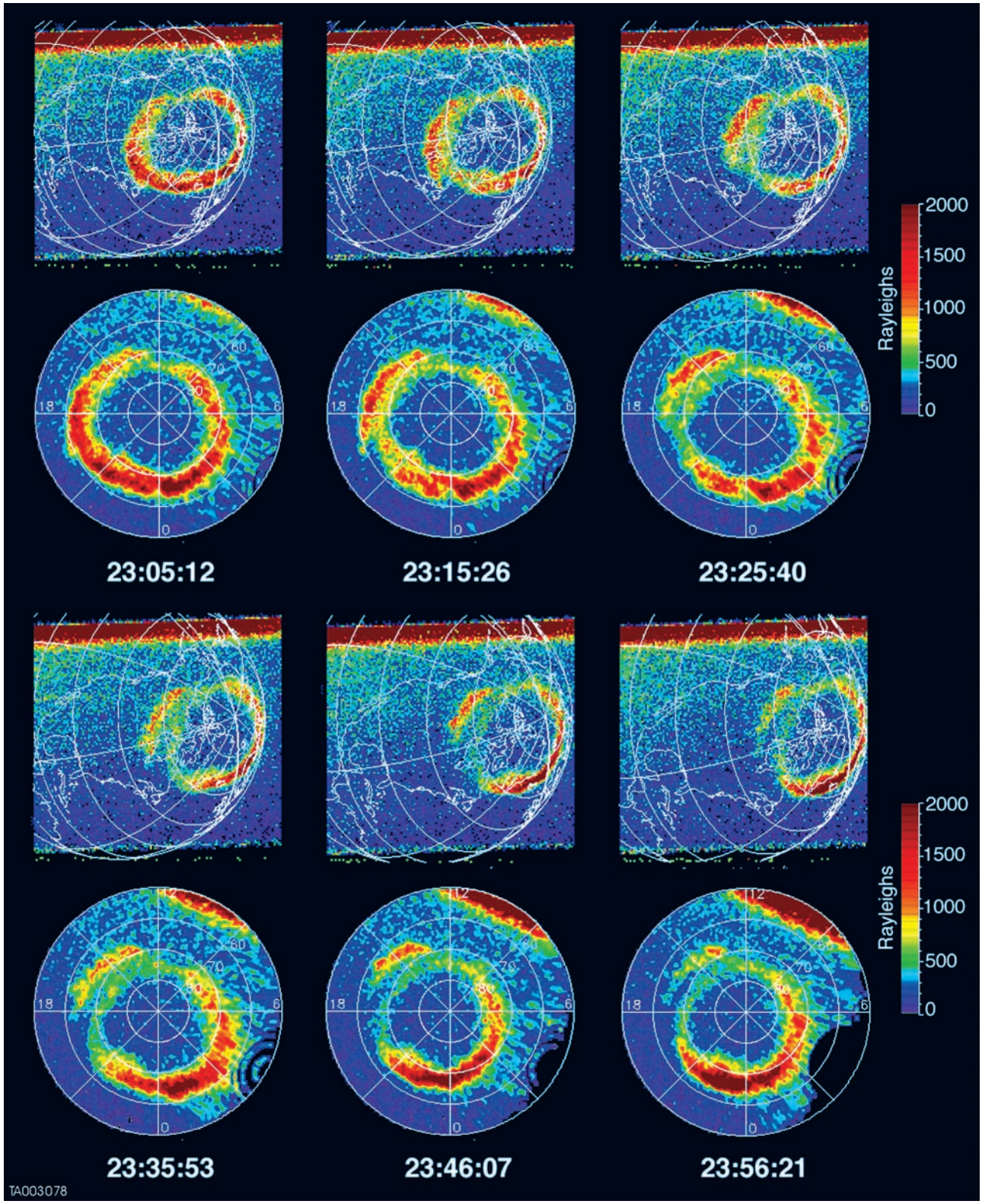

Figure 6. Time series showing the evolution of the detached proton arc on 23 January 2001. As noted in the text, the arc persists until at least 0224:59 UT, after which the spacecraft began its perigee pass and could not image the northern auroral region for ~3.5 hours. As in Figure 1, the false color gives the emission intensity in Rayleighs.

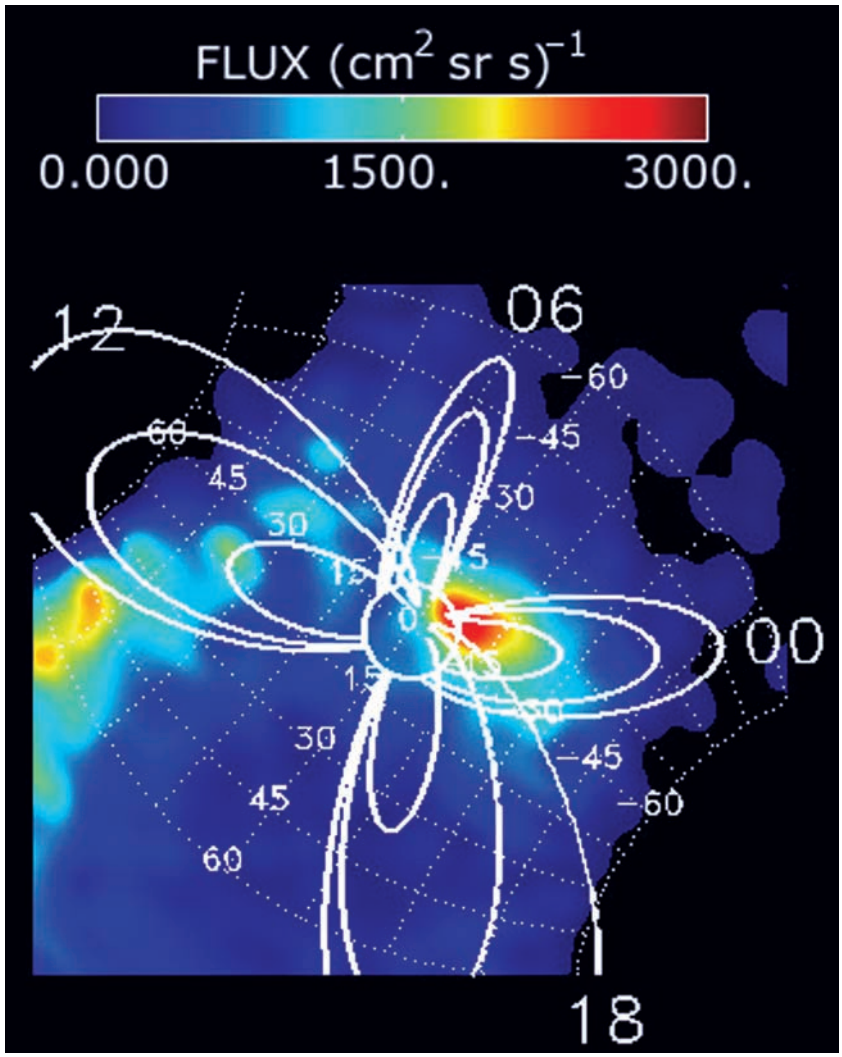

Figure 7. HENA data acquired during the 23 January event, between 2324:31 UT and 2326:32 UT. The format is the same as in Figure 2. The view is from approximately dusk toward the Earth. The satellite was at a geocentric distance of 6.2 R_E.

substorm recovery phase, when *AE* was decreasing from a maximum value of ~550 nT. HENA images were also obtained during this event (Figure 7) and, as in the case of the 9–10 November arc, showed an energetic neutral atom distribution typical of substorm injections, with strong emissions from midnight extending into the early morning hours and toward the dusk meridian. (The emissions seen near the noon meridian in the HENA images are produced by sunlight contamination).

[14] The 23–24 January arc event is discussed by *Immel et al.* [2002], who showed FAST data from the conjugate Southern Hemisphere location of the arc, demonstrating that the arc was associated with ion precipitation and that the electron precipitation was very weak. DMSP northern hemisphere data for this event, presented in Figure 8, are consistent with the results of Immel et al. and show a proton precipitation pattern identical to that sketched above for the 9–10 November event, with higher-energy proton precipitation above the detached arc and lower-energy protons over the main oval. The purpose of showing data from this same event here is to illustrate the dynamic effect that occurs when B_y changes from negative to positive, causing the main proton oval to move poleward in the afternoon sector, causing a detachment of the proton arc.

[15] ACE solar wind data for January 23, 2001 are shown in Figure 9. As in the case of the 9–10 November event, the solar wind dynamic pressure is enhanced, with n_p = 18.76 cm^{-3} and V_{sw} = 470.31 km s^{-1}; and the magnetosphere is compressed, with the calculated stagnation point moved inward to 6.9 R_E. Higher time-resolution (16 s) IMF data are presented in Figure 10. In both figures, the shaded region shows the time period (after correction for the transit time from ACE) over which the proton arc became detached from the main oval. In Figure 6 only every fifth image from the selected time interval is shown, but this time resolution is sufficient to show the detachment of the proton arc, which (as in the 9–10 November event) begins with the development of a spur feature near 1930 MLT in the first image. We note in Figure 10 that IMF B_y was negative during the first half of the shaded region and strongly positive over most of the second half before again turning negative near the end of the period. Examination of the series of images in Figure 6

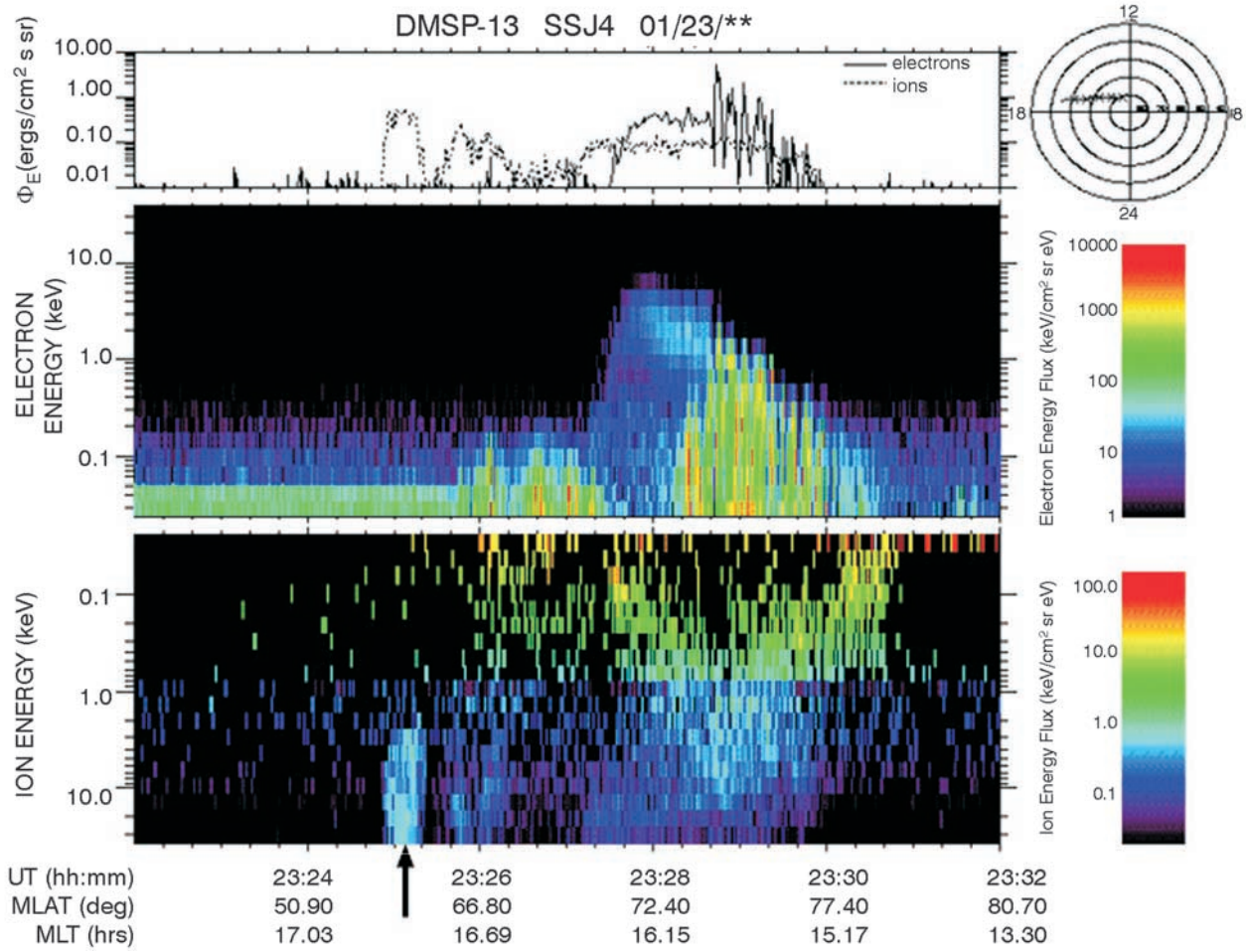

Figure 8. DMSP data acquired during the 23 January 2001 event. As in Figure 5, a black arrow identifies the ion feature associated with the subauroral arc.

reveals again that the detached proton arc closely maintains its position in Λ and MLT while the main proton oval in the afternoon sector moves poleward by several degrees. As the arc detachment develops, the arc becomes more localized toward earlier local times as can be seen in the 9–10 November event in Figure 1. A well-defined detached arc is still present at 0024:59 UT on 24 January, when the spacecraft begins its perigee pass, during which useful images are not available. (Once IMAGE has ascended from perigee and attained an altitude from which the auroral oval and dayside subauroral latitudes are again visible in the FUV field of view, at 0445:32 UT, a detached subauroral arc can be seen at approximately the same location as the feature at 0024:59 UT. This arc, not shown here, remains clearly distinguishable from the background until about 0515 UT. Because of the lack of images during the perigee pass, it cannot be determined whether the arc seen at 0445:32 UT and subsequently is a continuation of the event that began on 23 January or a new arc that developed during the ~3.5-hour period when FUV could not see the northern auroral zone.)

3. Discussion

[16] The two events presented above show how proton auroras resident in the equatorward part of the auroral oval can develop into subauroral arcs in the afternoon sector when the IMF rotates either from southward to northward or from westward to eastward. Similar arcs may also result from other processes. For example, IMAGE FUV-SI data from 8 June 2000 show the rapid appearance of a short-lived subauroral afternoon-sector proton arc within one imaging period (two minutes) of the arrival of an interplanetary shock at the magnetosphere [*Fuselier et al.*, 2001]. That event demonstrates that it is not necessary for the proton arc to appear first in the equatorward part of the main oval and then move away from the arc as in the 9–10 November 2000 and 23–24 January 2001 events discussed in the previous sections. Instead, the arc location apparently can be set up by previous variations in the IMF with precipitation occurring later, in association with a magnetospheric compression.

[17] Considering the case of the detached proton arc on 9–10 November 2000, the separation of the arc from the proton oval appears to follow the following sequence: (1) substorm ion injection and drift through the dusk-side hemisphere; (3) precipitation of protons in the 1200–2000 MLT sector; (3) positioning of the resulting proton auroras along the equatorward half of the main proton auroral oval, with the higher-latitude emissions mapped to the boundary layer and/or magnetopause; (4) a rapid

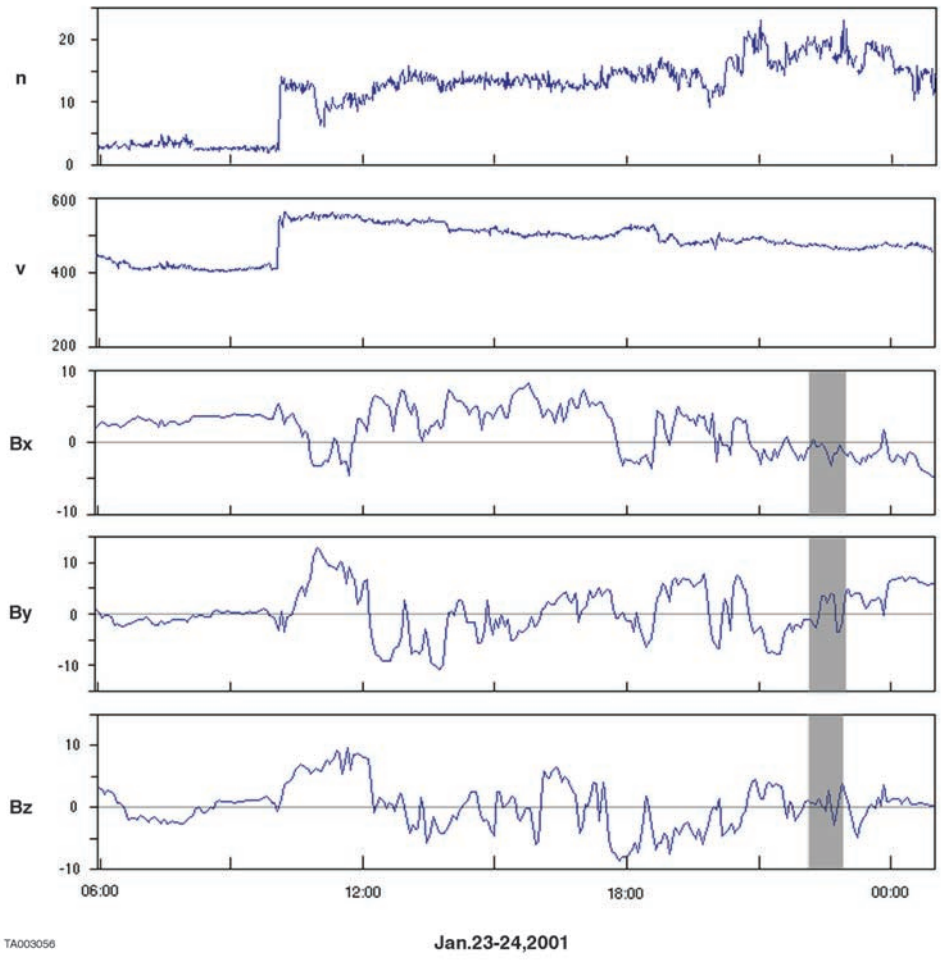

Figure 9. Solar wind data from ACE. IMF data are 4-min averages. Shaded region shows times covered by FUV-SI images in Figure 6 (after correction for estimated one-hour travel time between ACE and the magnetosphere).

rotation of the IMF from southward to northward causing a immediate poleward contraction of the oval (and outward motion of the magnetopause); and (5) development of a gap between the oval and the ring current proton arc and shrinking of the arc toward the dayside as the injection of new protons ceases or the level of turbulence in the duskside magnetosphere diminishes.

[18] The proposed sequence for the 23–24 January 2001 case is similar except that in this case the IMF rotation is from west to east rather than from south to north, and the FUV-SI images show the primary motion of the proton oval to be a poleward contraction but only in the afternoon sector. Based on data from Dynamics Explorer 1, *Burch et al.* [1985] suggested high-latitude convection patterns for B_y positive (east) and negative (west) that predict this type of oval contraction in the afternoon sector for $B_y > 0$. A similar pattern was deduced by *Cowley et al.* [1991]. An important element of these proposed patterns is the alignment of sunward and antisunward convection paths along the oval in the afternoon sector for $B_y < 0$. In contrast, the convection paths in this region for $B_y > 0$ are generally normal to the oval, and the convection reversal is located at a higher latitude [see *Cowley et al.*, 1991, Figure 3]. The images in Figure 6 thus represent a confirmation of this latter prediction of these models.

[19] In both cases presented here, the subauroral emissions became more localized in the mid-afternoon sector as auroral activity decreased. Similar subauroral proton emissions have been observed with the FUV/SI12 in this same general region (i.e., within 2 hours in MLT of 1500 and between 60° and 70° Λ) on other occasions. As illustrated by the observations for June 8 mentioned above, these do not necessarily evolve from the main oval, and there is no evident association between their occurrence and changes in the IMF orientation. What we wish to call attention to here, however, is an apparent tendency for dayside subauroral emissions to occur preferentially in a location that maps to the midafternoon sector of the magnetosphere from near geosynchronous orbit out to the magnetopause. During and following periods of enhanced geomagnetic activity, this region of the magnetosphere contains a plume of eroded plasmaspheric material that extends toward the magnetopause [e.g., *Elphic et al.*, 1996]; and the localized precipitation of protons observed in the midafternoon sector may result from the interaction of hot plasma sheet or ring current plasma with this cooler plasmaspheric material.

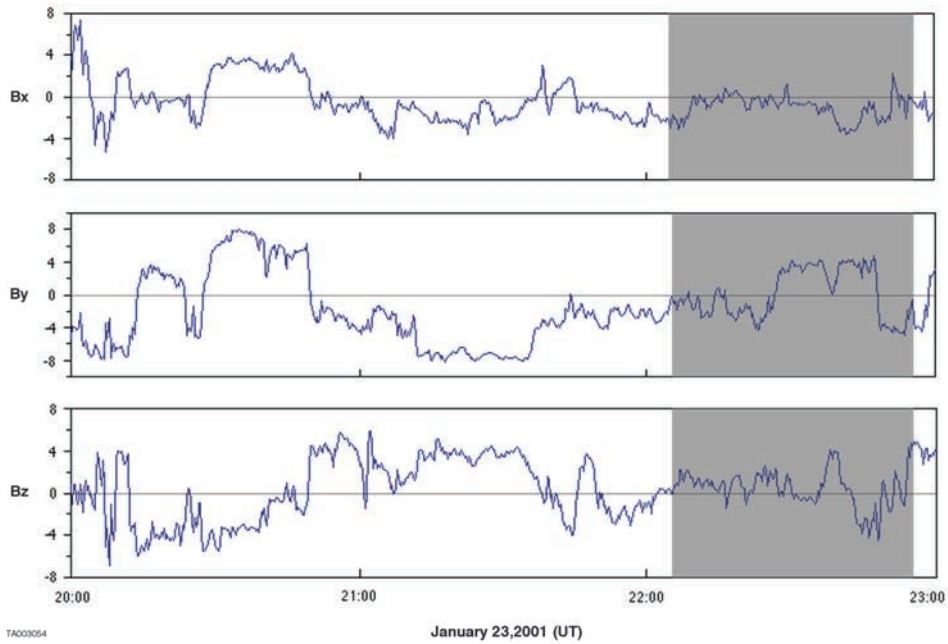

Figure 10. ACE 16-s IMF data for 23 January 2001. Shaded region denotes times of images in Figure 6 (after correction for estimated one-hour travel time between ACE and the magnetosphere).

[20] Was a plasmaspheric drainage plume present at the time of the two events? Such plumes are frequently seen in the images of the plasmasphere obtained with the IMAGE Extreme Ultraviolet (EUV) imager, which detects 30.4 nm photons resonantly scattered by the singly ionized helium component of the plasmasphere [*Sandel et al.*, 2000; *Burch et al.*, 2001; *Sandel et al.*, 2001]. Unfortunately, no useful EUV data were taken during either event. However, the existence of plasmaspheric material in the midafternoon sector of the magnetosphere at the time of the subauroral arc event on 9–10 November is indicated by particle data from geosynchronous spacecraft 1989-046. This spacecraft crossed through the expected equatorial extension of the detached proton arc at the same universal time as the DMSP low-altitude crossing and at an earlier local time (~1330 UT) where, according to the image in Figure 1, the arc's location was at a latitude (67°) that is expected to map to geosynchronous orbit. The 1989-046 data are shown in Figure 11, which shows plasma sheet and ring current proton fluxes at energies from a few keV to >20 keV and also shows low-energy plasmaspheric ions at energies generally below 10 eV. However, at the time of the expected crossing of the proton arc, the plasmaspheric ions are accelerated to a few tens of eV, and throughout this region and on either side of it a strong ~10-min oscillation is seen in the low-energy ion fluxes. As shown in Figure 11, this oscillation has the form of a vortical right-handed velocity rotation with frequency in the Pc5 range. Such oscillations are commonly observed in the geosynchronous data but have not yet been explained.

[21] Detached subauroral arcs possibly related to those described here were observed in the evening sector with the ISIS 2 Auroral Scanning Photometer (ASP) at 557.7 and 391.4 nm [*Anger et al.*, 1978; *Moshupi et al.*, 1979]. The arcs were observed between 60° and 70° invariant latitude, the majority between 1500 and 1800 MLT. The arcs appeared not to be correlated with *Dst* or *Kp* but did appear to be associated with subsiding substorm activity as indicated by a decrease in *AE*. Moreover, the occurrence of the arcs showed a clear correlation with a change in B_z from south to north; no such correlation was found for B_y [*Moshupi et al.*, 1979]. The association of the arcs with a northward turning of B_z and a reduction in substorm activity led Moshupi et al. to attribute them to "plasma sheet particles injected during magnetic storms or substorms and left behind by a poleward retreat of the auroral oval." Based on the analysis of ISIS 2 particle data, *Wallis et al.* [1979] concluded that the particles responsible for the arcs were predominantly residual plasma sheet electrons; proton precipitation in the arc region was observed only rarely, and then together with electron precipitation. Wallis et al. proposed that the electron precipitation resulted from interactions with cold plasmaspheric material in the form either of plumes or detached plasma regions.

[22] There are strong similarities between the detached arcs described by *Moshupi et al.* [1979] and those discussed in this paper. Both are observed in the same general Λ-MLT sector; both appear to occur during the substorm recovery phase. Like the detached arcs seen in the ISIS 2 data, the 9–10 November event was associated with a poleward contraction of the main oval resulting from a northward turning of B_z. However, while *Moshupi et al.* [1979] found no significant association of arc occurrence with B_y, such a dependence is indicated by the SI12 observations of the 23–24 January detachment event. Finally, as shown by the analysis of *Immel et al.* [2002] and by the DMSP data presented in this paper (Figures 5 and 8), the subauroral arcs observed with the SI12 instrument result unambiguously from proton precipitation; no electron fluxes above 500 eV are seen in the particle data corresponding to these

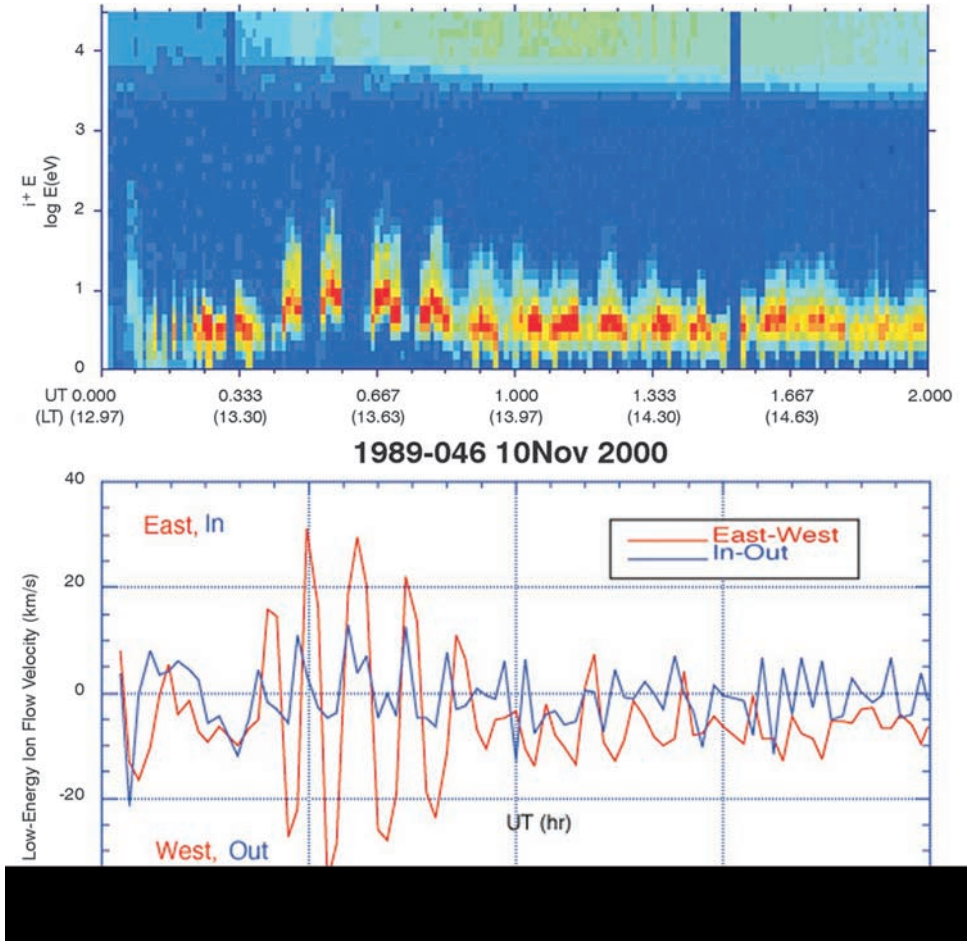

Figure 11. Low-energy particle data from the Magnetospheric Plasma Analyzer on 10 November 2000, from geosynchronous spacecraft 1989-046. Data are for the first 2 hours of the day and for the 1300–1500 MLT sector of the magnetosphere.

events. It is not clear how to reconcile this result with the conclusion of *Wallis et al.* [1979] that precipitating protons do not play a significant role in the production of the detached arcs. We note, however, that emissions at the two wavelengths at which the arcs were observed with the ISIS 2 ASP, 557.7 and 391.4 nm, can be excited by precipitating protons as well as by energetic electrons [*Eather*, 1967]. Nonetheless, the ISIS 2 evidence for energetic electrons as the particles responsible for the subauroral emissions remains to be accounted for. Indeed, it is possible that two types of subauroral arcs can occur, one dominated by protons and one excited by electrons.

[23] In addition to the ISIS 2 observations of detached arcs, there has been at least one ground-based observation of a subauroral proton precipitation feature in the dusk sector. A "drifting spot of diffuse aurora" was observed at wavelengths of 557.7 and 486.1 nm (Hβ) by *Ono et al.* [1987] from Syowa Station. The spot was located equatorward of the main oval at $\Lambda \sim 65°$ in the dusk sector and was drifting westward at a speed of $\sim$0.4 km s^{-1}. DMSP data available for the event indicated that the spot was caused by proton precipitation. Ono et al. call attention to the similarity between this "structured proton aurora" and the detached arcs reported by *Anger et al.* [1978], although they note that the spot and the detached arcs differ in longitudinal extent. The ground-based observation by Ono et al. is too limited in its spatial and temporal coverage to permit comparison of the drifting spot with the subauroral arcs seen with the FUV/SI12 instrument.

4. Conclusions

[24] We have presented two afternoon-sector detached proton arc events that were identified in images from the IMAGE FUV-SI instrument. In both cases, proton precipitation along the equatorward part of the auroral oval developed into a detached proton arc in the afternoon sector. In both cases, the arc did not move appreciably, but became detached because of a poleward contraction of the oval. In the first case (on 9–10 November 2000), the detachment was associated with a rotation of the IMF from southward to northward, causing a poleward contraction of the entire oval. In the second case (on 23–24 January 2001), the detachment was associated with a rotation of the IMF from westward to eastward, causing the poleward contraction of the afternoon sector of the oval. The dynamics of the oval in both of these cases was consistent with existing models of the IMF control of the interaction of the solar wind with the magnetosphere. While the poleward contraction of the entire oval in response to IMF northward turnings is well

known, the data for the 23 January 2001 event may represent the first confirmation of the prediction of the poleward motion of the oval in the afternoon sector in response to a negative to positive rotation of the dominant IMF *y* component by *Burch et al.* [1985].

[25] For both events, proton precipitation at energies of several keV to a few tens of keV was confirmed using data from simultaneous overflights of the DMSP-13 satellite. In the case of the 9–10 November event, geosynchronous satellite data further confirmed the mapping of the detached arc to the ring current and to a plasmaspheric drainage plume and showed an accompanying strong vortical oscillation in the plasmaspheric ion velocity distributions with a period near ten minutes. We note that a precipitation feature whose morphology resembles that of the detached arcs is seen in the statistical study of proton precipitation by *Hardy et al.* [1989] in the same MLT sector in which the arcs are observed. In contrast to the observations presented here, this feature appears only for extremely disturbed conditions ($Kp \geq 6$) [cf. *Hardy et al.*, 1989, Plates 1b and 2b]. This difference notwithstanding, however, it is clear that in both the statistical study and the SI12 proton aurora images a region has been identified in which strong subauroral proton precipitation preferentially occurs. The mechanism responsible for the subauroral precipitation likely involves the interaction of hot ring current or plasma sheet ions with cold plasmaspheric material; and the enhanced solar wind dynamic pressure observed during the events reported here suggests that magnetospheric compression may be a predisposing condition for this interaction, perhaps through an enhancement of electromagnetic ion cyclotron wave activity as suggested by *Anderson and Hamilton* [1993]. However, the exact nature of the mechanism responsible for the proton precipitation and the conditions under which it is triggered are not clear. The answers to these questions will require additional particle and wave data in the equatorial magnetosphere.

[26] **Acknowledgments.** Support for this research was provided by NASA contract NAS5-96020 with Southwest Research Institute. J.C.G. is supported by the Belgian National Fund for Scientific Research (FNRS) and the Fund for Collective Fundamental Research (grant FRFC 97-2.4569.97). The Belgian participation in the IMAGE mission is funded by the PRODEX program of the European Space Agency. Research at Lockheed-Martin is supported by subcontract with the University of California at Berkeley. Work at Los Alamos was conducted under the auspices of the U.S. Department of Energy. Principal investigators for the SWEPAM and MAG instruments on ACE are D. J. McComas and N. F. Ness, respectively; the principal investigator for the SOHO CELIAS instrument is P. Bochsler. A. Ridley provided the quasi-*AE* data for the 23–24 January event. Quicklook *AE* data for the 9–10 November event were obtained from the World Data Center in Kyoto, Japan, and were derived by T. Kamei.

References

Anderson, B. J., and D. C. Hamilton, Electromagnetic ion cyclotron waves stimulated by modest magnetospheric compressions, *J. Geophys. Res.*, *98*, 11,369, 1993.

Anger, C. D., et al., Detached auroral arcs in the trough region, *J. Geophys. Res.*, *83*, 2683, 1978.

Burch, J. L., IMAGE Mission overview, *Space Sci. Rev.*, *91*, 1, 2000.

Burch, J. L., et al., Views of Earth's magnetosphere with the IMAGE satellite, *Science*, *291*, 619, 2001.

Burch, J. L., et al., IMF By-dependent plasma flow and Birkeland currents in the dayside magnetosphere, I, Dynamics Explorer observations, *J. Geophys. Res.*, *90*, 1577, 1985.

Cowley, S. W. H., et al., Dependence of convective flows and particle precipitation in the high-latitude dayside ionosphere on the *X* and *Y* components of the interplanetary magnetic field, *J. Geophys. Res.*, *96*, 5557, 1991.

Eather, R. H., Auroral proton precipitation and hydrogen emissions, *Rev. Geophys.*, *5*, 207, 1967.

Elphic, R. C., et al., Evolution of plasmaspheric ions at geosynchronous orbit at times of high geomagnetic activity, *Geophys. Res. Lett.*, *23*, 2189, 1996.

Frank, L. A., and J. D. Craven, Imaging results from Dynamics Explorer 1, *Rev. Geophys.*, *26*, 249, 1988.

Frey, H. U., et al., The electron and proton aurora as seen by IMAGE-FUV and FAST, *Geophys. Res. Lett.*, *28*, 1135, 2001.

Fuselier, S. A., et al., Ion outflow observed by IMAGE: Implications for source regions and heating mechanisms, *Geophys. Res. Lett.*, *28*, 1163, 2001.

Fuselier, S. A., et al., Cusp aurora dependence on interplanetary magnetic field B_z, *J. Geophys. Res.*, *107*, 10.1029/2001JA900165, in press, 2002.

Gérard, J. C., et al., Observation of the proton aurora with IMAGE-FUV and simultaneous ion flux in-situ measurements, *J. Geophys. Res.*, *106*, 28,939, 2001.

Gussenhoven, M. S., D. A. Hardy, and N. Heinemann, Systematics of the equatorward diffuse auroral boundary, *J. Geophys. Res.*, *88*, 5692, 1983.

Gvozdevsky, B. B., V. A. Sergeev, and K. Mursula, Long lasting energetic proton precipitation in the inner magnetosphere after substorms, *J. Geophys. Res.*, *102*, 24,333, 1997.

Hardy, D. A., M. S. Gussenhoven, and D. Brautigam, A statistical model of auroral ion precipitation, *J. Geophys. Res.*, *94*, 370, 1989.

Immel, T. J., et al., Precipitation of auroral protons in detached arcs, *Geophys. Res. Lett.*, *107*, 10.1029/2001GL013847, *29*(11), 1519, 2002.

Lorentzen, D. A., and J. Moen, Auroral proton and electron signatures in the dayside aurora, *J. Geophys. Res.*, *105*, 12,733, 2000.

Meinel, A. B., Doppler-shifted auroral hydrogen emission, *Astrophys. J.*, *113*, 50, 1951.

Mende, S. B., et al., Far ultraviolet imaging from the IMAGE spacecraft, 3, Spectral imaging of Lyman-α and OI 135.6 nm, *Space Sci. Rev.*, *91*, 287, 2000.

Mende, S. B., et al., Global observations of proton and electron auroras in a substorm, *Geophys. Res. Lett.*, *28*, 1139, 2001.

Miller, J. R., and B. A. Whalen, Characteristics of auroral proton precipitation from sounding rockets, *J. Geophys. Res.*, *81*, 147, 1976.

Mitchell, D. G., et al., High-energy neutral atom (HENA) imager for the IMAGE mission, *Space Sci. Rev.*, *91*, 67, 2000.

Moshupi, M. C., et al., Characteristics of trough region auroral patches and detached arcs observed by ISIS 2, *J. Geophys. Res.*, *84*, 1347, 1979.

Ono, T., T. Hirasawa, and C. I. Meng, Proton auroras observed at the equatorward edge of the duskside auroral oval, *Geophys. Res. Lett.*, *14*, 660, 1987.

Sanchez, E., et al., Low-altitude observations of the evolution of substorm injection boundaries, *J. Geophys. Res.*, *98*, 5815, 1993.

Sandel, B. R., et al., The extreme ultraviolet imager investigation for the IMAGE mission, *Space Sci. Rev.*, *91*, 197, 2000.

Sandel, B. R., et al., Initial results from the IMAGE extreme ultraviolet imager, *Geophys. Res. Lett.*, *28*, 1439, 2001.

Strickland, D. J., et al., Midcourse Space Experiment/Ultraviolet and Visible Imaging and Spectrographic Imaging limb observations of combined proton/hydrogen/electron aurora, *J. Geophys. Res.*, *106*, 65, 2001.

Takahashi, Y., and H. Fukunishi, The dynamics of the proton aurora in auroral breakup events, *J. Geophys. Res.*, *106*, 45, 2001.

Vegard, L., Hydrogen showers in the auroral region, *Nature*, *144*, 1089, 1939.

Vegard, L., Emission spectra of the night sky and aurora, report of the Gassiot Committee, 82 pp., Phys. Soc. of London, London, 1948.

Wallis, D. D., et al., Observations of particles precipitating into detached arcs and patches equatorward of the auroral oval, *J. Geophys. Res.*, *84*, 1347, 1979.

P. C. Anderson, Aerospace Corporation, El Segundo, CA 90245, USA.

J. L. Burch and W. S. Lewis, Southwest Research Institute, San Antonio, TX 78228, USA. (wlewis@swri.edu)

H. U. Frey, T. J. Immel, and S. B. Mende, University of California, Berkeley, CA 94720, USA.

S. A. Fuselier, Lockheed Martin Advanced Technology Center, Palo Alto, CA 94304, USA.

J.-C. Gérard, University of Liège, Liège, B 4000, Belgium.

D. G. Mitchell, Applied Physics Laboratory, Johns Hopkins University, Laurel, MD 21218, USA.

M. F. Thomsen, Los Alamos National Laboratory, Los Alamos, NM 87545, USA.